



OPEN

Reduction of parasitic reaction in high-temperature AlN growth by jet stream gas flow metal–organic vapor phase epitaxy

Kentaro Nagamatsu^{1,2}, Shota Tsuda², Takumi Miyagawa², Reiya Aono², Hideki Hirayama^{1,3}, Yuusuke Takashima² & Yoshiki Naoi^{1,2}

AlGaIn-based deep ultraviolet light-emitting diodes (LEDs) have a wide range of applications such as medical diagnostics, gas sensing, and water sterilization. Metal–organic vapor phase epitaxy (MOVPE) method is used for the growth of all-in-one structures, including doped layer and thin multilayers, using metal–organic and gas source raw materials for semiconductor devices. For AlN growth with high crystalline quality, high temperature is necessary to promote the surface migration of Al atoms and Al-free radicals. However, increase in temperature generates parasitic gas-phase prereactions such as adduct formation. In this work, AlN growth at 1500 °C by a stable vapor phase reaction has been achieved by jet stream gas flow metal–organic vapor phase epitaxy. The AlN growth rate increases with gas flow velocity and saturates at ~ 10 m/s at room temperature. Moreover, it is constant at an ammonia flow rate at a V/III ratio from 50 to 220. These results demonstrate the reduction in adduct formation, which is a typical issue with the vapor phase reaction between triethylaluminum and ammonia. The developed method provides the in-plane uniformity of AlN thickness within 5%, a low concentration of unintentionally doped impurities, smooth surface, and decrease in dislocation density because of the suppression of parasitic reactions.

AlGaIn-based deep ultraviolet LEDs have a wide range of applications such as medical diagnostics, gas sensing, biochemical agent detection, and water sterilization. Such devices enable the sterilization of home appliances, which are in high demand in the market^{1,2}. Recently, deep ultraviolet LEDs have been proposed as a system for reliable sterilization of items from SARS-CoV-2^{3–5}. However, a large cooling system for deep ultraviolet LED is required for heat dissipation in known devices because a lot of input power is converted to heat owing to the low efficiency of LEDs². The heat generation is caused by dislocation and point defect nonradiative recombination^{6–9}. Metal–organic vapor phase epitaxy (MOVPE) method provides the growth of all-in-one structures, including doped layers and thin multilayers, using metal–organic and gas source raw materials. All semiconductor devices, including LED, LD, and electron devices are manufactured using this method. The growth of the AlN underlying layer for DUV-LEDs is an essential problem for the MOVPE method.

For growing AlN with high crystalline quality, high temperature is necessary to promote the surface migration of Al atoms and Al-free radicals^{10–13}.

There are two reaction pathways: an adduct formation by Al and N sources, or a TMAI pyrolysis reaction.

However, the increase in temperature generates parasitic gas-phase prereactions such as adduct formation by TMAI and ammonia, as shown in Fig. 1. The parasitic reactions not only cause waste of source gas but also seriously affect the level of unintentionally doped impurities, growth uniformity, and generation of dislocations^{10–13}.

Figure 1 shows the schematic representation of raw material transport in a growth reactor. The supplied TMAI raw material forms Al or Al–H at the substrate surface by a pyrolysis reaction, as shown in Eq. (1) and Al–N adduct by parasitic reaction or contaminant particles by polymerization, as shown by Eq. (2).



¹Institute of Post-LED Photonics, Tokushima University, 2-1 Minami-josanjima, Tokushima 770-8506, Japan. ²Graduate School of Advanced Technology and Science, Tokushima University, 2-1 Minami-josanjima, Tokushima 770-8506, Japan. ³RIKEN, Institute of Physical and Chemical Research, Wako 351-0198, Japan. ✉email: nagamatsu@tokushima-u.ac.jp

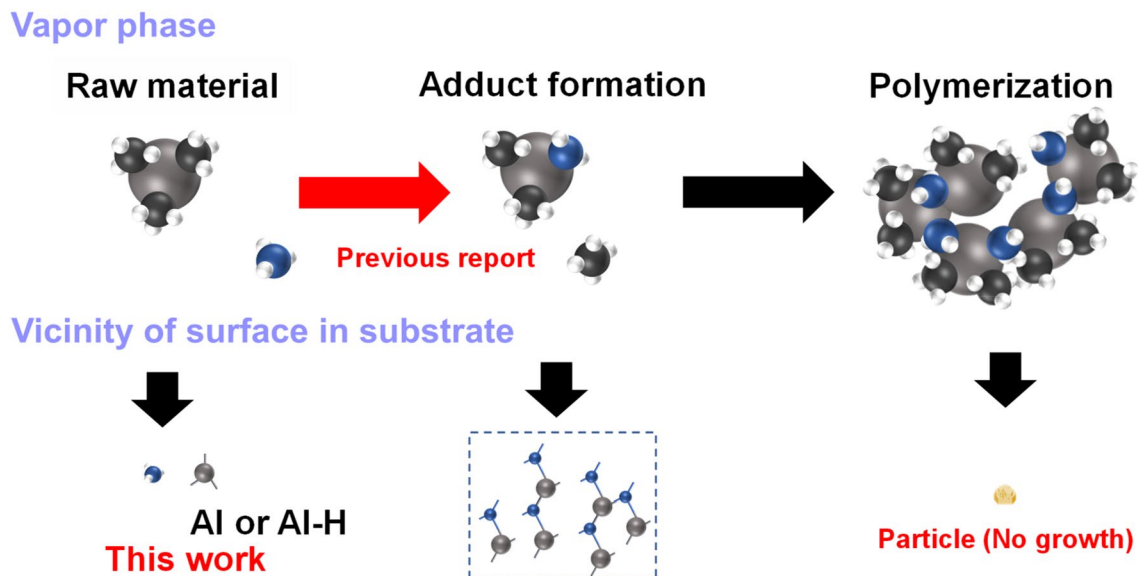
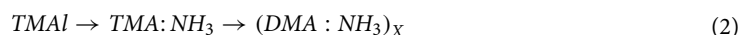


Figure 1. Reaction pathway during raw material transport at AlN growth, and the estimation of final material condition before its deposition on an AlN surface.



As per a previous report, the adduct formation is unavoidable at TMAI reaction with NH_3 during the HT-MOCVD process^{10,11}. A state of Al–N chemical compound, which is a typical source for AlN growth, is not ideal. The products of nitrogen prereaction with Al–N obstruct the surface migration of Al atoms. Al or Al–H formed by the pyrolysis reaction without the reaction of ammonia possesses a large migration range on the substrate surface¹⁴. However, adduct polymerization depletes the source materials because particle contamination prevents crystal growth. This problem may be resolved by an alternative supply method from aluminum and nitrogen sources, as reported by Adivarahan et al. and in other works^{15–18}. This method not only suppresses the parasitic reaction but also enhances Al migration over the substrate surface; however, it is difficult to increase the growth rate in principle.

Similarly, a growth method with a low NH_3 flow rate was reported with the suppressed parasitic reaction^{19–21}. This technique enabled maintaining the growth rate by reducing NH_3 supply despite the high temperature. However, metallic Al is deposited at an NH_3 flow rate below a minimum value. Therefore, the parasitic reaction was strongly suppressed; however, the process was difficult to control in a wider temperature range, e.g., at a temperature of > 1500 °C. Thus, these parasitic reactions in the vapor phase unavoidably occur during AlN growth at high temperatures and high growth rates^{10–13}. Therefore, the growth method had to be optimized.

In this study, parasitic reactions were eliminated in the designed and manufactured MOVPE reactor with a high-speed gas flow where gas turbulence was avoided using a mechanism of the combustion chamber in a jet engine. Hence, AlN crystal growth at a high temperature without the parasitic reaction was provided with a low concentration of impurities and a smooth surface.

Results and discussion

A jet engine operating system continuously performs the gas intake, compression, combustion, and exhaustion from the inlet, i.e., a combustion reactor provides a high-temperature laminar gas flow with a high velocity. A combustion chamber comprises a combustion part in the center where fuel burns by mixing with compressed oxygen, whereas the outside bulk is separated by a wall composed of Ti alloy with perforations that provide compressed air inflow and prevent the wall from overheating (Fig. 2a).

Consequently, the chamber wall can be composed of Ti alloy with a lower melting point compared to the temperature in the combustion part heated at > 2000 °C. Moreover, the compressive air is supplied with a controllable speed to the chamber through holes in this wall.

A horizontal-type MOVPE usually uses two or three multilayer flow channels as the gas inlet. The velocity of supply gas flow is determined by the channel cross-section, temperature, and pressure. Hydrogen gas flow from the inlet to the substrate surface (upper-side flow) was provided in our MOVPE reactor by analogy to a jet engine combustion chamber, as shown in Fig. 2b. Figure 2c shows a schematic representation of the MOVPE reactor used in this study. The gas flow increases step by step in the reactor at the same rate as that of the jet gas flow. Tantalum carbide-coated carbon was used as the material of the reactor with an increase in high temperature for safety. The gas flow in conventional MOVPE occurred through three inlet at the maximum on the left-hand side. Therefore, there is one more factor determining the gas flow velocity in this reactor. The MOVPE reactor should be kept clean. Hydrogen gas was selected for the upper-side flow. Moreover, the upper-side gas flow system provides additional options in the selection of heat-resistant materials for the upside flow channel.

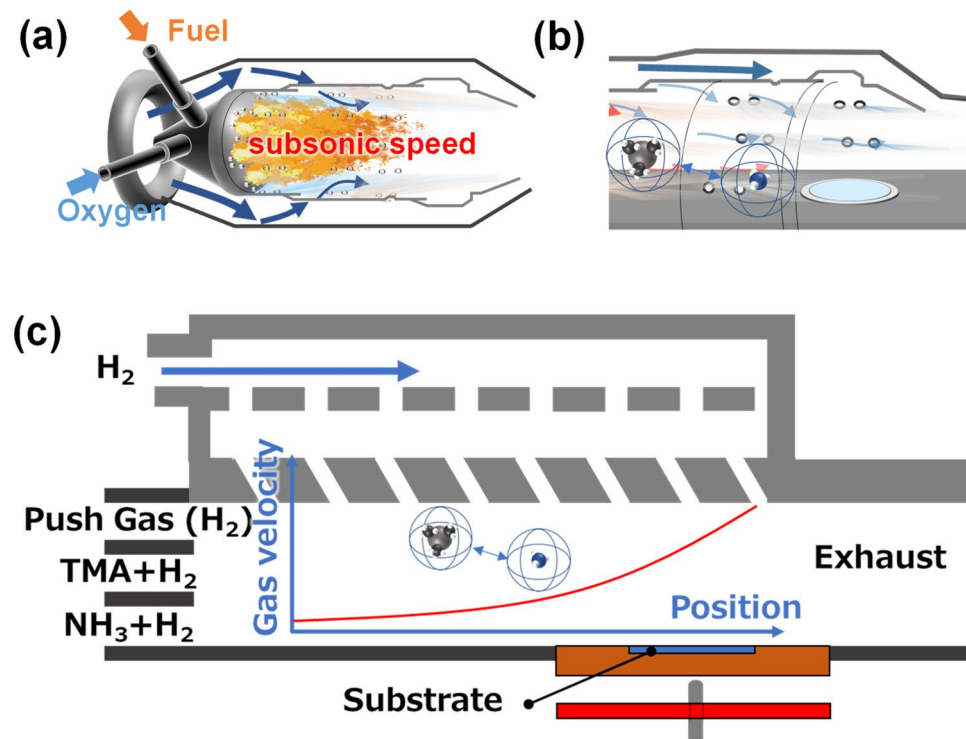


Figure 2. Schematic representation of the growth reactor involving gas flow from the jet engine. (a) The heating area in the combustion chamber of a jet engine. The temperature in this chamber exceeds 2000 °C (b) An image of raw materials gas flow in the combustion chamber. (c) The metal–organic vapor phase epitaxy reactor developed in this study, mimicking a combustion chamber in a jet engine.

Figure 3a shows the growth rate at 1500 °C as a function of gas flow velocity at room temperature. The total gas flow velocity increases owing to the reinforcement of the upper-side gas flow. The growth rate increased with total gas flow velocity and saturated at ~ 10 m/s. These results show that the parasitic reaction of the supply material occurs in a weak gas flow. The in-plane thickness uniformity was within 5%. In particular, the material source depletes to < 50% at a gas flow of < 5 m/s, and the dominant type of the supplied raw material are particles that do not contribute to growth. The gas flow velocity in a conventional MOVPE should be 1–2 m/s to provide nonturbulent flow and maintain the substrate^{22,23}. Clearly, a high-temperature growth, e.g., at 1500 °C, is complicated because a higher gas flow velocity is necessary. The discussed gas velocities are indicated at room temperature, while actual gas flow velocity at high temperatures should be higher. For example, 15 m/s at room temperature corresponds to 101 m/s on the substrate upside surface at 1500 °C as per our calculations. The quantity of growth material in the microspace increased to provide the reaction without adduct formation in the vapor phase.

The adduct formation by the parasitic reaction is theoretically unavoidable in the case of simultaneous supply with TMAI and NH_3 ^{10–13}. In other words, the reaction is determined by the probability of the contact between Al and N. Moreover, the growth rate is affected by the parasitic reaction^{19,20}.

The obtained surface morphology was affected by the parasitic reaction. Under the condition of 20% loss of growth material with the gas flow velocity of 10 m/s, the atomic step by sapphire disorientation angle is clearly observed using an atomic force microscope in Fig. 3c. However, the surface has macrowaves, curved atomic steps, and microconvexity in the center in contrast to the image taken at 16.5 m/s (Fig. 3b). Moreover, the terrace length uniformity was clearly improved (Fig. 3b,c and 3c) with the reduction of the parasitic reaction. The X-ray full width at half maximum value for (0002) and (10–12) diffractions of grown AlN layer were 250 and 580 arcsec, respectively, in the sample in Fig. 3c, and 160 and 310 arcsec, respectively, in the sample in Fig. 3b.

The effect of parasitic reaction on the AlN growth rate was examined at different TMAI flow rates (Fig. 4a). AlN growth rate linearly increases up to 8 $\mu\text{m}/\text{h}$ with the TMAI flow rate, unlike previous studies^{20,21}, where the growth rate saturated at ~ 1 $\mu\text{m}/\text{h}$ owing to a parasitic reaction. Hence, the dependence in Fig. 4b shows that the increased NH_3 flow rate impedes the transportation of Al compound by promoting the parasitic reaction. Therefore, in^{19–21}, the growth rate decreased with increasing NH_3 content. Our results show that the parasitic reaction does not occur at V/III ratios from 50 to 220 (Fig. 4b).

The low concentrations of oxygen, silicon, and carbon impurities in films should be demonstrated to confirm the advantages of the proposed growth process. In particular, the oxygen concentration was reported to affect optical properties by forming oxygen-vacancy complexes; hence, reduction of its concentration is important²⁴. Moreover, oxygen is always generated upon sapphire (Al_2O_3) heating. The oxygen concentration decreases with an increase in gas flow velocity (Fig. 5a). This phenomenon can be explained by the quick exhaustion of generated oxygen. The data on admixture concentrations in AlN obtained in this work and reported in the literature are demonstrated in Fig. 5b. Importantly, the concentrations of all impurities in AlN grown in this study are lower

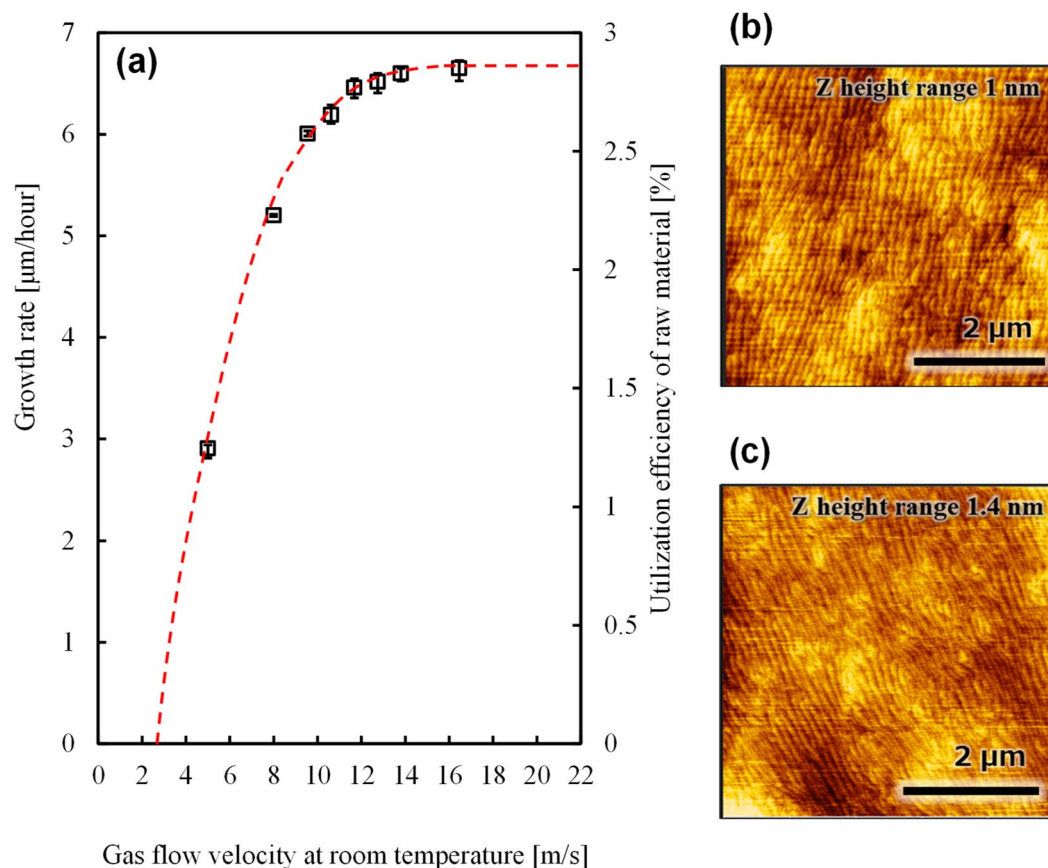


Figure 3. Effect of gas flow velocity. (a) The growth rate of AlN layer as a function of gas velocity calculated at room temperature. The adduct formation and polymerization decreased the amount of raw material used for the growth at flow rates below 10 m/s; (b) Atomic force microscope (AFM) images of AlN film grown at a gas flow velocity of 10 m/s. The growth rate in the experiment was approximately 20% lower under these conditions compared to the values presented in (a); (c) AFM images of AlN surface grown at a gas flow velocity of 16.5 m/s.

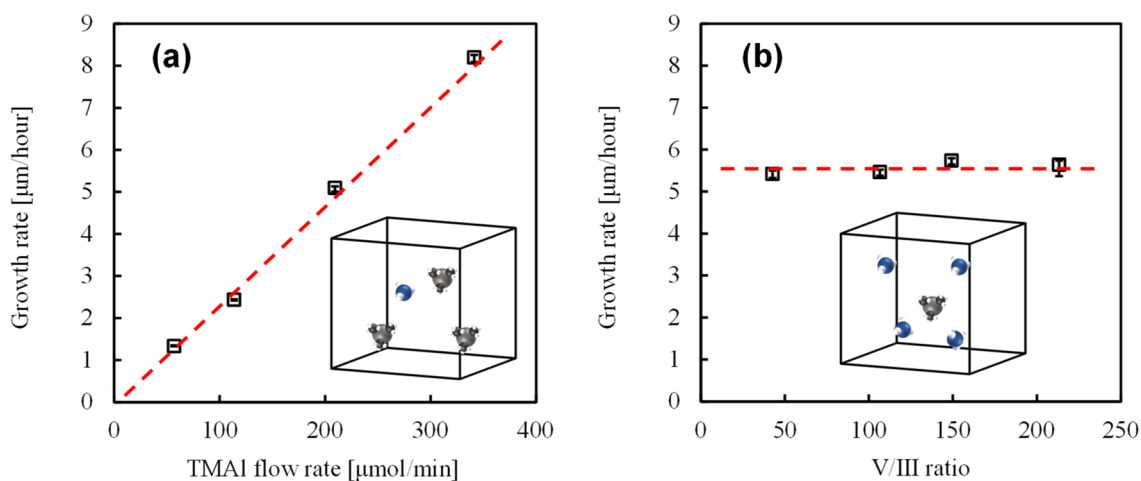


Figure 4. Evidence of suppressed parasitic reaction at an increasing growth rate at a gas flow velocity of 16.5 m/s. (a) AlN growth rate vs. TMAI flow rate. Increasing Al source concentration in certain areas result in adduct formation and growth rate saturation; (b) Dependence of AlN growth rate on ammonia flow rate. Increasing N source concentration in a certain area increases the adduct formation probability, similar to (a). The growth rate decreases with an increasing ammonia flow rate in the case of adduct formation.

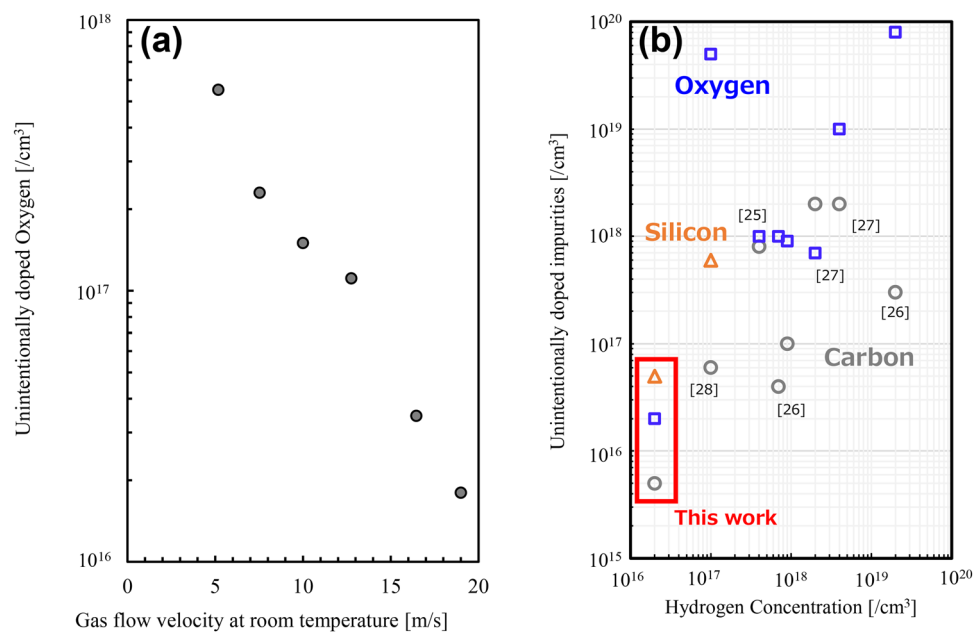


Figure 5. The impurity concentrations ingrown AlN. **(a)** Oxygen admixture concentration in the AlN measured using secondary ion mass spectrometry (SIMS) as the function of gas flow velocity grown under fixed growth temperature of 1500 °C. This figure demonstrates the efficiency of increasing gas flow for the reduction of oxygen concentration. The data were obtained at a depth of around 500 nm below the crystal surface; **(b)** Comparison between the best data impurity concentrations measured by SIMS obtained in this work compared to those reported in the literature^{25–28}.

by how many orders of magnitude compared with those reported in previous studies^{25–28}. A high temperature of 1500 °C and a high gas velocity of 16.5 m/s provided such impurity concentrations. The reduction in carbon impurities are similar to that of GaN, and the methyl group of transport materials decompose with an increase in temperature. Then, the carbon impurities reduce because of the decomposed methyl group forming methane²⁹.

Moreover, conventional MOVPE system uses quartz at the flow channel. In that case, Si impurities are contaminations from the quartz material that decomposed at > 1200 °C. Our system was cooling the upper side flow-channel as the highest temperature region by the jet stream gas flow. Moreover, our equipment did not contain quartz. Consequently, the concentration of the unintentional Si impurities is considerably less.

To summarize, we designed and manufactured an MOVPE reactor providing stable crystal growth even at high gas flow velocities. The growth rate of AlN on the sapphire substrate increased by increasing the gas flow velocity. The process of AlN growth by MOVPE with a high gas flow velocity effectively reduces the parasitic reaction between TMAI and ammonia. Consequently, a low concentration of unintentionally doped impurities and smooth film surface were obtained because of the suppression of this parasitic reaction. Finally, the reduction in dislocation density was confirmed by XRD.

Method

AlN layers were grown on the (0001) sapphire substrate using the horizontal type MOVPE with a jet engine gas flow system. The misorientation of the sapphire substrate from m-plane was 0.2°. The reactor was coated with carbonized tantalum to ensure thermal and corrosion resistance. This equipment can withstand temperatures of up to 2000 °C. The growth of AlN was attributed to the continuous flow of TMA carrier gas and ammonia; herein, TMAI and ammonia were used as Al and N precursors, respectively. The growth rate was primarily determined using the TMA flow rate, as the ammonia flow rate was a hundred times faster. Hydrogen was used in the reactor without ammonia as a carrier gas and a heater and reactor purge gas to avoid molecular nitrogen pyrolysis. The growth temperature was simultaneously measured using a thermocouple and dual-wavelength pyrometer to control the pyrometer indications. Firstly, 5-nm thick AlN buffer layers were deposited at 950 °C. Secondly, 650-nm thick first AlN layers were grown at 1500 °C to guarantee stable crystalline quality. Then, the second AlN layers were grown on the first layers. The standard growth process temperature and duration were 1500 °C and 30 min, respectively. The TMA and NH₃ flow rates were 209 μmol/min and 45 mmol/min, respectively.

The gas flow velocities at room temperature were calculated using the following equation.

$$\text{Flow velocity}(R.T) = \frac{F}{A} \times \frac{P_G}{101.3kPa} \quad (3)$$

where F is the total flow rate, A is the cross-section area, P_G is the growth pressure in the reactor. The gas flow velocities at the growth temperature of 1500 °C were calculated by computational fluid dynamics analysis (simulation).

The atomic layer and surface roughness in AlN were measured by AFM (HITACHI corporation 5500 M). To measure the crystalline quality, X-ray diffraction rocking curve measurement was obtained at Smart Lab (Rigaku Corporation). Moreover, the FWHM of XRD data was confirmed, and the correlation with dislocation densities using a transmission electron microscope provided by the Foundation for Promotion of Material Science and Technology of Japan (MST) was obtained. SIMS measurement was measured by MST, and AlN growth thickness was measured by an optical interference film thickness meter.

Data availability

The data that support the findings of this study are available from the corresponding author upon reasonable request.

Received: 1 November 2021; Accepted: 14 April 2022

Published online: 10 May 2022

References

- Oguma, K., Kita, R., Sakai, H., Murakami, M. & Takizawa, S. Application of UV light emitting diodes to batch and flow-through water disinfection systems. *Desalination* **328**, 24–30 (2013).
- Song, K., Mohseni, M. & Taghipour, F. Application of ultraviolet light-emitting diodes (UV-LEDs) for water disinfection: A review. *Water Res.* **94**, 341–349 (2016).
- Liu, S. *et al.* Sec-Eliminating the SARS-CoV-2 by AlGaIn based high power deep ultraviolet light source. *Adv. Funct. Mater.* **31**, 200802. <https://doi.org/10.1002/adfm.202008452> (2020).
- Inagaki, H., Saito, A., Sugiyama, H., Okabayashi, T. & Fujimoto, S. Rapid inactivation of SARS-CoV-2 with deep-UV LED irradiation. *Emerg. Microbes Infect.* **9**, 1744–1747 (2020).
- Minamikawa, T. *et al.* Quantitative evaluation of SARS-CoV-2 inactivation using a deep ultraviolet light-emitting diode. *Sci. Rep.* **11**, 1–9 (2021).
- Kneissl, M., Seong, T. Y., Han, J. & Amano, H. The emergence and prospects of deep ultraviolet light emitting diode technologies. *Nat. Photon.* **13**, 233–244 (2019).
- Hirayama, H. Quaternary InAlGaIn-based high-efficiency ultraviolet light-emitting diodes. *J. Appl. Phys.* **97**, 091101. <https://doi.org/10.1063/1.1899760> (2005).
- Shatalov, M. *et al.* AlGaIn deep-ultraviolet light-emitting diodes with external quantum efficiency above 10%. *Appl. Phys. Express* **5**, 082101. <https://doi.org/10.1143/apex.5.082101> (2012).
- Ban, K. *et al.* Internal quantum efficiency of whole-composition-range AlGaIn multiquantum wells. *Appl. Phys. Express* **4**, 052101. <https://doi.org/10.1143/apex.4.052101> (2011).
- An, J., Dai, X., Zhang, Q., Guo, R. & Feng, L. Gas-phase chemical reaction mechanism in the growth of AlN during high-temperature MOCVD: A thermodynamic study. *ACS Omega* **5**, 11792–11798 (2020).
- Zhang, H., Zuo, R., Zhong, T. & Zhang, L. Quantum chemistry study on gas reaction mechanism in AlN MOVPE growth. *J. Phys. Chem. A* **124**, 2961–2971 (2020).
- Mihopoulos, T. G., Gupta, V. & Jensen, K. F. A reaction-transport model for AlGaIn MOVPE growth. *J. Cryst. Growth* **195**, 733–739 (1998).
- Matsumoto, K. & Tachibana, A. Growth mechanism of atmospheric pressure MOVPE of GaN and its alloys: Gas phase chemistry and its impact on reactor design. *J. Cryst. Growth* **272**, 360–369 (2004).
- Sekiguchi, K. *et al.* Thermodynamic considerations of the vapor phase reactions in III-nitride metal organic vapor phase epitaxy. *Jpn. J. Appl. Phys.* **56**, 04CJ04. <https://doi.org/10.7567/jjap.56.04cj04> (2017).
- Adivarahan, V. *et al.* 250 nm AlGaIn light-emitting diodes. *Appl. Phys. Lett.* **85**, 2175–2177 (2004).
- Jain, R. *et al.* Migration enhanced lateral epitaxial overgrowth of AlN and AlGaIn for high reliability deep ultraviolet light emitting diodes. *Appl. Phys. Lett.* **93**, 051113. <https://doi.org/10.1063/1.2969402> (2008).
- Qhalid Fareed, R. S. *et al.* Migration enhanced MOCVD (MEMOCVD/MTM) buffers for increased carrier lifetime in GaN and AlGaIn epilayers on sapphire and SiC substrate. *Phys. Status Solidi C* **2**, 2095–2098 (2005).
- Nagamatsu, K. *et al.* Atomic layer epitaxy of AlGaIn. *Phys. Status Solidi C* **7**, 2368–2370 (2010).
- Imura, M. *et al.* Annihilation mechanism of threading dislocations in AlN grown by growth form modification method using V/III ratio. *J. Cryst. Growth* **300**, 136–140 (2007).
- Lovanova, A. V. *et al.* Effect of V/III ratio in AlN and AlGaIn MOVPE. *J. Cryst. Growth* **287**, 601 (2006).
- Zhao, D. G. *et al.* Parasitic reaction and its effect on the growth rate of AlN by metalorganic chemical vapor deposition. *J. Cryst. Growth* **289**, 72–75 (2006).
- Tokunaga, H. *et al.* Performance of multiwafer reactor GaN MOCVD system. *J. Cryst. Growth* **221**, 616–621 (2000).
- Kwon, M. S. & Cho, S. I. Effects of total gas velocity during growth of undoped GaN epitaxial layer on sapphire (0 0 1) substrate by horizontal MOCVD. *J. Cryst. Growth* **266**, 435–440 (2004).
- Uedono, A. *et al.* Vacancy-oxygen complexes and their optical properties in AlN epitaxial films studied by positron annihilation. *J. Appl. Phys.* **105**, 054501. <https://doi.org/10.1063/1.3079333> (2009).
- Li, X.-H. *et al.* Growth of high-quality AlN layers on sapphire substrates at relatively low temperatures by metalorganic chemical vapor deposition. *Phys. Status Solidi B* **252**, 1089–1095 (2015).
- Imura, M. *et al.* Impact of high-temperature growth by metal-organic vapor phase epitaxy on microstructure of AlN on 6H-SiC substrates. *J. Cryst. Growth* **310**, 2308–2313 (2008).
- Kakanakova-Georgieva, A., Nilsson, D. & Janzen, E. High-quality AlN layers grown by hot-wall MOCVD at reduced temperatures. *J. Cryst. Growth* **338**, 52–56 (2012).
- Kuboya, S. *et al.* Crystalline quality improvement of face-to-face annealed MOVPE-grown AlN on vicinal sapphire substrate with sputtered nucleation layer. *J. Cryst. Growth* **545**, 125722. <https://doi.org/10.1016/j.jcrysgro.2020.125722> (2020).
- Nagamatsu, K. *et al.* Decomposition of trimethylgallium and adduct formation in a metalorganic vapor phase epitaxy reactor analyzed by high-resolution gas monitoring system. *Phys. Status Solidi B* **8**, 1600737. <https://doi.org/10.1002/pssb.201600737> (2017).

Acknowledgements

This work was partially supported by JSPS KAKENHI Grant-in-Aid for Challenging Exploratory Research Number 20K21006 and The Project on the Promotion of Regional Industries and Universities, Cabinet Office.

Author contributions

K.N. wrote the main manuscript text and figure. All authors discussed the contents of the manuscript and reviewed the manuscript.

Competing interests

The authors declare no competing interests.

Additional information

Correspondence and requests for materials should be addressed to K.N.

Reprints and permissions information is available at www.nature.com/reprints.

Publisher's note Springer Nature remains neutral with regard to jurisdictional claims in published maps and institutional affiliations.



Open Access This article is licensed under a Creative Commons Attribution 4.0 International License, which permits use, sharing, adaptation, distribution and reproduction in any medium or format, as long as you give appropriate credit to the original author(s) and the source, provide a link to the Creative Commons licence, and indicate if changes were made. The images or other third party material in this article are included in the article's Creative Commons licence, unless indicated otherwise in a credit line to the material. If material is not included in the article's Creative Commons licence and your intended use is not permitted by statutory regulation or exceeds the permitted use, you will need to obtain permission directly from the copyright holder. To view a copy of this licence, visit <http://creativecommons.org/licenses/by/4.0/>.

© The Author(s) 2022